Electronic Supplementary Material (ESI) for ChemComm.

Supporting Information

Synthesis and reactivity of iron–dinitrogen complexes bearing anionic methyl- and phenyl-substituted pyrrole-based PNP-type pincer ligands toward catalytic nitrogen fixation

Yoshiya Sekiguchi, Shogo Kuriyama, Aya Eizawa, Kazuya Arashiba, Kazunari Nakajima, and Yoshiaki Nishibayashi*

Department of Systems Innovation, School of Engineering, The University of Tokyo, Bunkyo-ku, Tokyo 113-8656, Japan

General Methods.

^{1}H NMR (400 MHz), ^{31}P{^{1}H} NMR (162 MHz), and ^{13}C NMR (101 MHz) spectra were recorded on a JEOL ECS-400 spectrometer in suitable solvent, and spectra were referenced to residual solvent (^{1}H and ^{13}C{^{1}H}) or external standard (^{31}P{^{1}H}: H_3PO_4). IR spectra were recorded on a JASCO FT/IR 4100 Fourier transform infrared spectrometer. Magnetic susceptibility was measured in solution by using Evans' method.[1-3] Absorption spectra were recorded on a Shimadzu MultiSpec-1500. Evolved dihydrogen was quantified by gas chromatography using a Shimadzu GC-8A with a TCD detector and a SHINCARBON ST (6 m 3 mm). Elemental analyses were performed at Microanalytical Center of The University of Tokyo.

All manipulations were carried out under an atmosphere of nitrogen by using standard Schlenk techniques or glovebox techniques unless otherwise stated. Solvents were dried by general methods, and degassed before use. 3,4-dimethylpyrrole,[4] 2,5-bis(dimethylaminomethyl)-3,4-diphenylpyrrole,[5] $[FeCl_2(thf)_{1.5}]$ (thf = tetrahydrofuran),[6] KC_8,[7] and $[H(OEt_2)_2][BAr^F_4]$ (Ar^F = 3,5-$(CF_3)_2C_6H_3$)[8] were prepared according to the literature method. **3a** was prepared according to the previous paper,[9] and the crystals suitable for X-ray crystallography was obtained by recrystallization from Et_2O/hexane. All the other reagents were commercially available.

Preparation of 2,5-bis(dimethylaminomethyl)-3,4-dimethylpyrrole.

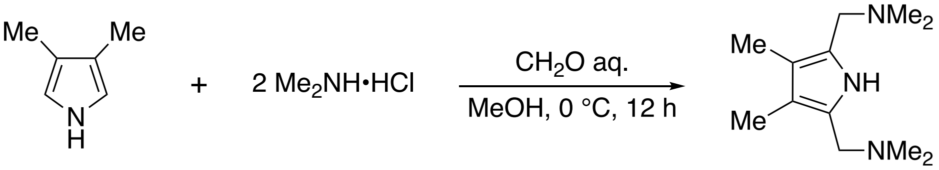

3,4-Dimethylpyrrole (0.419 g, 4.40 mmol), dimethylamine hydrochloride (0.790 mg, 9.69 mmol) and formaldehyde solution (37% in H_2O, 1 mL) were dissolved in MeOH (5 mL), and then the solution was stirred at 0 °C for 12 h. To the resultant black solution was slowly added a solution of NaOH (1.75 M in H_2O, 10 mL) at 0 °C. After the solution was extracted with Et_2O, the organic layer was dried over anhydrous sodium sulfate, filtered and evaporated to afford black oil. The crude compound was purified by sublimation to give the title compound as a yellow solid (435 mg, 2.08 mmol, 47%).

^{1}H NMR ($CDCl_3$): 8.15 (s, N*H*, 1H), 3.32 (s, C*H*$_2$NMe$_2$, 4H), 2.19 (s, CH$_2$N*Me*$_2$, 12H), 1.94 (s, *Me*, 6H). ^{13}C {^{1}H} NMR ($CDCl_3$): 123.7, 115.4, 54.5, 45.1, 9.0. Anal. Calcd. for $C_{12}H_{23}N_3$: C, 68.85; H, 11.07; N, 20.07. Found: C, 68.90; H, 10.98; N, 19.68. M.p. = 49.2-51.0 °C.

Preparation of 2,5-bis(di-*tert*-butylphosphinomethyl)-3,4-dimethylpyrrole.

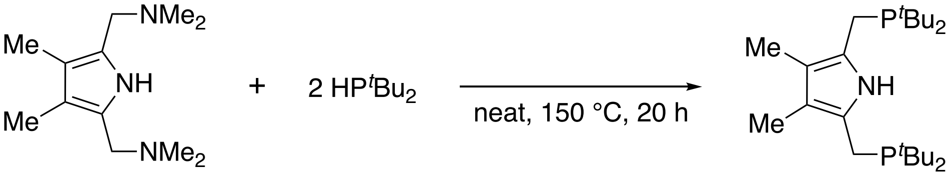

A mixture of 2,5-bis(dimethylaminomethyl)-3,4-dimethylpyrrole (587 mg, 2.80 mmol) and di-*tert*-butylphosphine (870 mg, 5.95 mmol) was stirred at 150 °C for 20 h. All volatiles were removed *in vacuo* to afford dark brown oil (826 mg, 2.01 mmol, 72 %), which was used in the next reaction without further purification.

^{1}H NMR (C_6D_6): 8.55 (s, N*H*, 1H), 2.74 (s, CH_2P^{t}Bu$_2$, 4H), 2.13 (s, *Me*, 6H), 1.05 (d, $J_{\text{P-H}}$ = 10.5 Hz, CH$_2$P^t*Bu$_2$*, 36H). ^{31}P{^{1}H} NMR (C_6D_6): 21.3 (s).

Preparation of 2,5-bis(di-*tert*-butylphosphinomethyl)-3,4-diphenylpyrrole.

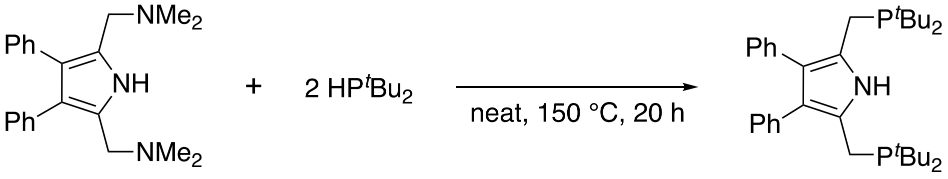

2,5-Bis(dimethylaminomethyl)-3,4-diphenylpyrrole (621 mg, 1.86 mmol) and di-*tert*-butylphosphine (567 mg, 3.88 mmol) was mixed and stirred at 150 °C for 20 h. All volatiles were removed *in vacuo* to afford dark brown oil (927 mg, 1.73 mmol, 93%), which was used in the next reaction without further purification.

^{1}H NMR (C_6D_6): 9.40 (s, N*H*, 1H), 7.45-7.42 (m, *Ph*, 4H), 7.20-7.16 (m, *Ph*, 4H), 7.04-7.00 (m, *Ph*, 2H), 3.01 (s, CH_2P^{t}Bu$_2$, 4H), 0.99 (d, $J_{\text{P-H}}$ = 10.5 Hz, CH$_2$P^t*Bu$_2$*, 36H). ^{31}P{^{1}H} NMR (C_6D_6): 23.2 (s).

Preparation of lithium 2,5-bis(di-*tert*-butylphosphinomethyl)-3,4-diphenylpyrrolide (Ph-PNP-Li).

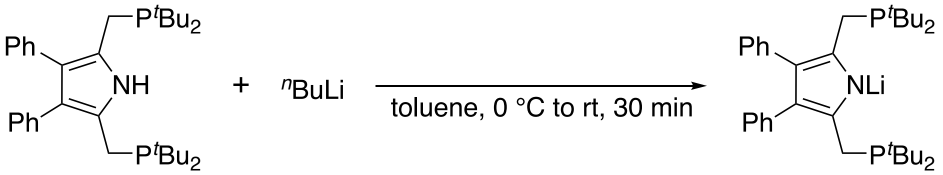

Ph-PNP-Li

To a solution of 2,5-bis(di-*tert*-butylphosphinomethyl)-3,4-diphenylpyrrole (4.06 g, 7.58 mmol) in toluene (15 mL) was added dropwise *n*BuLi (1.60 M in hexane, 5.20 mL, 8.32 mmol) at 0 °C. The reaction mixture was stirred at room temperature for 30 min, and the solvent was removed *in vacuo*. The obtained solid was washed with pentane and dried *in vacuo* to afford Ph-PNP-Li as a white solid (3.03 g, 5.59 mmol, 74%).

^{1}H NMR (THF-d_8): 7.00-6.99 (m, C$_5$*H$_6$*, 8H), 6.82-6.76 (m, C$_5$*H$_6$*, 2H), 3.05 (s, CH_2P^{t}Bu$_2$, 4H), 0.97 (d, $J_{\text{P-H}}$ = 10.1 Hz, CH$_2$ P^t*Bu$_2$*, 36H). ^{31}P{^{1}H} NMR (THF-d_8): 22.1 (s). Anal. Calcd. for $C_{34}H_{50}LiNP_2$: C, 75.39; H, 9.30; N, 2.59. Found: C,75.69; H, 9.49; N, 2.85.

Preparation of [FeCl(Me-PNP)] (2b).

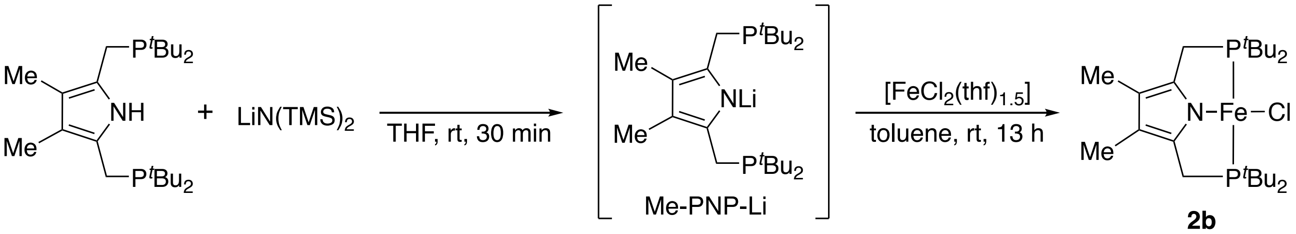

To a solution of 2,5-bis(di-*tert*-butylphosphinomethyl)-3,4-dimethylpyrrole (826 mg, 2.01 mmol) in THF (8 mL) was added 1.3 M lithium bis(trimethylsilyl)amide THF solution (1.6 mL), and then the resulting black mixture was stirred at room temperature for 1 h. After the solvent was removed *in vacuo*, toluene (8 mL) was added. To the resultant black solution was added a suspension of [FeCl$_2$(thf)$_{1.5}$] (472 mg, 2.01 mmol) in toluene (8 mL). After stirring at room temperature for 13 h, the mixture was filtered through Celite and concentrated *in vacuo*. The residue was dissolved in benzene and to the solution was added pentane (2 mL) to give orange precipitate. The precipitate was collected by filtration, washed with pentane and dried *in vacuo* to give **2b** (416 mg, 0.830 mmol, 41%). Orange crystals of **2b** suitable for X-ray crystallography were obtained by recrystallization from Et$_2$O at -30 °C.

^{1}H NMR (C$_6$D$_6$): -9.56, -24.3. Magnetic susceptibility (Evans' method): $\mu_{\rm eff} = 3.9\pm0.1\ \mu_{\rm B}$ in C$_6$D$_6$ at 298 K. Anal. Calcd. for C$_{24}$H$_{46}$ClFeNP$_2$: C, 57.44; H, 9.24; N, 2.79. Found: C, 57.40; H, 9.07; N, 2.96.

Preparation of [FeCl(Ph-PNP)] (2c).

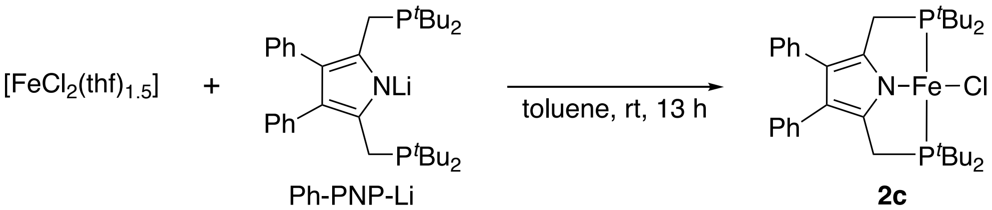

To a suspension of [FeCl$_2$(thf)$_{1.5}$] (137 mg, 0.581 mmol) in toluene (3 mL) was added a suspension of lithium 2,5-bis(di-*tert*-butylphosphinomethyl)-3,4-diphenylpyrrolide (358 mg, 0.661 mmol) in toluene (6 mL), and then the resultant orange mixture was stirred at room temperature for 13 h. Hexane (3mL) was added to the orange mixture and stirred at room temperature for a few minutes. The mixture was filtered through Celite, and concentrated to *ca.* 1 mL. Then, addition of hexane (3 mL) afforded the orange solid **2c**, which was collected by decantation, washed with hexane and dried *in vacuo* (286 mg. 0.456 mmol, 78%). Orange crystals of **2c** suitable for X-ray crystallography were obtained by recrystallization from Et$_2$O at -30 °C.

^{1}H NMR (C$_6$D$_6$): 24.9, 18.1, -7.2, -24.9. Magnetic susceptibility (Evans' method): $\mu_{\rm eff} = 3.7\pm0.1\ \mu_{\rm B}$ in C$_6$D$_6$ at 298 K. Anal. Calcd. for C$_{34}$H$_{50}$ClFeNP$_2$: C, 65.23; H, 8.05; N, 2.24. Found: C, 65.41; H, 7.97; N, 2.47.

Preparation of [FeN_2(Me-PNP)] (1b).

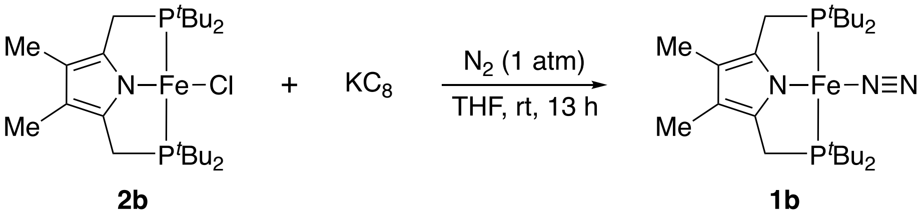

To a suspension of **2b** (42.7 mg, 0.0851 mmol) and KC_8 (22.2 mg, 0.164 mmol) in THF (4 mL) was stirred at room temperature for 13 h under N_2 (1 atm). The resultant black suspension was concentrated *in vacuo*. After the addition of toluene (3 mL) to the dark red residue, the solution was filtered through Celite. The filtrate was concentrated to *ca.* 0.5 mL and pentane (2 mL) was added to give **1b** as a dark purple solid, which were collected by filtration and dried *in vacuo* (14.6mg, 0.0295 mmol, 35%). Purple crystals of **1b** suitable for X-ray crystallography were obtained by recrystallization from Et_2O at -30 °C.

^1H NMR (C_6D_6): -1.89, -14.8. Magnetic susceptibility (Evans' method): $\mu_{eff} = 2.5\pm0.1\mu_B$ in C_6D_6 at 298 K. IR (KBr, cm^{-1}) 1959 (ν_{NN}). Anal. Calcd. for $C_{24}H_{46}FeN_3P_2$: C, 58.30; H, 9.38; N, 8.50. Found: C, 58.14; H, 9.18; N, 7.97.

Preparation of [FeN_2(Ph-PNP)] (1c).

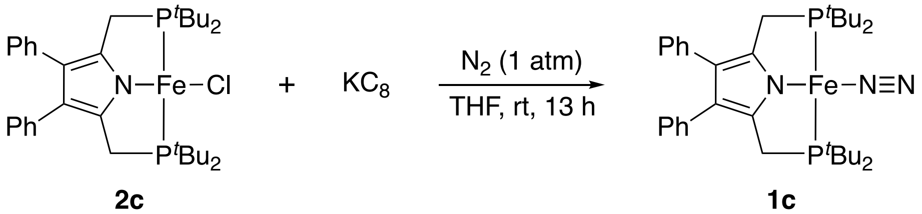

A suspension of **2c** (206 mg, 0.328 mmol) and KC_8 (82.2 mg, 0.608 mmol) in THF (6 mL) was stirred at room temperature for 13 h under N_2 (1 atm). The resultant black suspension was concentrated *in vacuo*. After the addition of Et_2O (5 mL) to the dark red residue, the solution was filtered through Celite. The filtrate was concentrated to *ca.* 1 mL and pentane (3 mL) was added to give **1c** as a dark purple solid, which were collected by decantation and dried *in vacuo* (72.0 mg, 0.116 mmol, 35%). Purple crystals of **1c** suitable for X-ray crystallography were obtained by recrystallization from Et_2O at -30 °C.

^1H NMR (C_6D_6): 10.9, 8.5, 8.2, -1.7. Magnetic susceptibility (Evans' method): $\mu_{eff} = 2.2\pm0.1\ \mu_B$ in C_6D_6 at 298 K. IR (KBr, cm^{-1}) 1969 (ν_{NN}). Anal. Calcd. for $C_{34}H_{50}FeN_3P_2$: C, 66.02; H, 8.15; N, 6.79. Found: C, 66.09; H, 8.07; N,6.22.

Catalytic Reduction of Molecular Dinitrogen into Ammonia and Hydrazine under N_2 (1 atm).

Catalytic reduction of molecular dinitrogen into ammonia was carried out in a modified experimental procedure of our previous work.[9] A typical experimental procedure using **1b** is described below. In a 50 mL Schlenk flask were placed **1b** (4.9 mg, 0.010 mmol), KC_8 (54.1 mg, 0.400 mmol), and $[H(OEt_2)_2]BAr^F{}_4$ (385 mg, 0.380 mmol) and then cooled to -78 °C. Cooled Et_2O (5 mL, -78 °C) was added to the mixture. After stirring at -78 °C for 1 h, the mixture was warmed to room temperature and further stirred at room temperature for 20 min. The amount of dihydrogen of the catalytic reaction was determined by GC analysis. The reaction mixture was evaporated under reduced pressure, and the distillate was trapped in dilute H_2SO_4 solution (0.5 M, 10 mL). Aqueous solution of potassium hydroxide (30 wt%, 5 mL) was added to the residue, and the mixture was distilled into another dilute H_2SO_4 solution (0.5 M, 10 mL). The amount of NH_3 present in each of the H_2SO_4 solutions was determined by the indophenol method.[10] The amount of N_2H_4 present in each of the H_2SO_4 solutions was determined by the *p*-(dimethylamino)benzaldehyde method.[11]

Supplementary Table 1. Iron-Catalyzed Reduction of Molecular Dinitrogen[a]

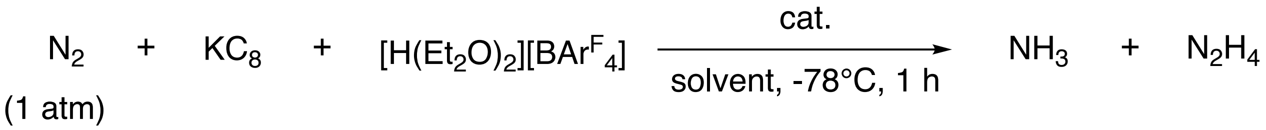

$$\underset{\text{(1 atm)}}{N_2} + KC_8 + [H(Et_2O)_2][BAr^F{}_4] \xrightarrow[\text{solvent, -78°C, 1 h}]{\text{cat.}} NH_3 + N_2H_4$$

run	cat.	solvent	KC_8 (equiv)[b]	$[H(OEt_2)_2][BAr^F{}_4]$ (equiv)[b]	NH_3 (equiv)[b]	N_2H_4 (equiv)[b]	H_2 (equiv)[b]
1	**1a**	Et_2O	40	38	4.7±0.9[c]	0.2±0.2[c]	2.6±1.0[c]
2	**1b**	Et_2O	40	38	5.0±0.8[c]	0.2±0.2[c]	3.0±0.2[c]
3	**1c**	Et_2O	40	38	3.7±0.6[c]	0.1±0.1[c]	3.8±1.4[c]
4	**3b**	Et_2O	40	38	5.3±0.2[c]	0.3±0.2[c]	3.6±0.4[c]
5	**1a**	Et_2O	200	184	11.6±0.5[c]	2.8±0.5[c]	23±1.0[c]
6	**1b**	Et_2O	200	184	22.7±1.7[c]	1.7±0.3[c]	21.0±2.4[c]
7	**1c**	Et_2O	200	184	4.7	1.2	29
8	**3b**	Et_2O	200	184	20.5±1.5[c]	1.7±1.7[c]	26.5±3.5[c]
9	**4b**	Et_2O	200	184	18	2.0	34
10	**1b**	Et_2O	400	368	17	1.9	67
11	**1a**	THF	80	76	2.0	0.9	9.1
12	**1b**	THF	80	76	1.7	0.2	11
13	**1c**	THF	80	76	1.3	0.4	11

[a] To a mixture of the catalysts, KC_8, and $[H(OEt_2)_2]BAr^F{}_4$ was added -78 °C Et_2O, and then the resultant mixture was stirred at -78 °C for 1 h. [b] Equiv based on the catalyst. [c] Average of multiple runs (>2 times) are shown.

Stoichiometric Reaction of 1b with $[H(OEt_2)_2][BAr^F_4]$ under N_2.

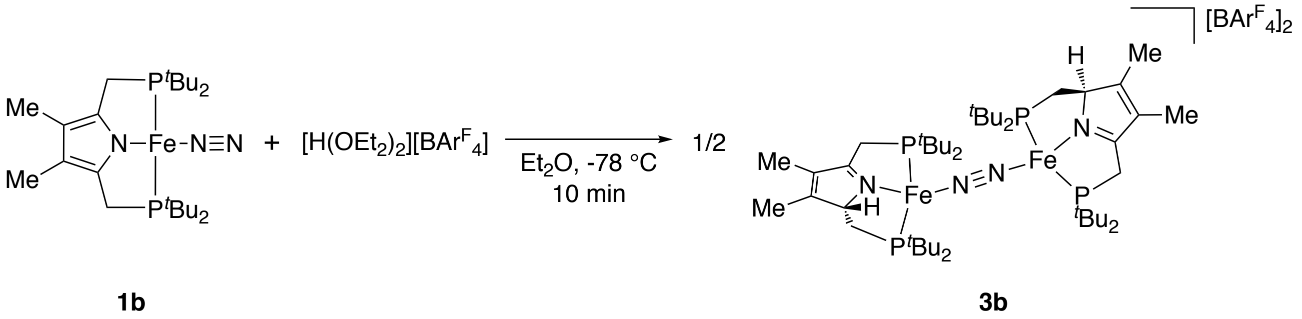

To a reddish purple solution of **1b** (20.1 mg, 0.041 mmol) in Et_2O (2 mL) at -78 °C was added a solution of $[H(OEt_2)_2][BAr^F_4]$ (41.3 mg, 0.041 mmol) in Et_2O (5 mL) at -78 °C and the resultant blue mixture was stirred at room temperature for 10 min under N_2 (1 atm). No formation of dihydrogen was confirmed by a GC. Addition of pentane (10 mL, -78 °C) to the reaction mixture afforded **3b** as a brown solid, which was collected by decantation and dried *in vacuo* (43.8 mg, 0.0163 mmol, 79%). Black crystals of **3b** suitable for X-ray crystallography were obtained by recrystallization from Et_2O/hexane. Magnetic susceptibility (Evans' method): $\mu_{eff} = 4.2\pm0.1$ μ_B in THF-*d8* at 298 K. IR (Et_2O, cm^{-1}) 2021 (ν_{NN}). Anal. Calcd. for $C_{112}H_{118}B_2F_{48}Fe_2N_4P_4$: C, 50.02; H, 4.42; N, 2.08. Found: C, 50.32; H, 4.41; N, 2.08.

Preparation of [FeH(Me-PNP)] (4b).

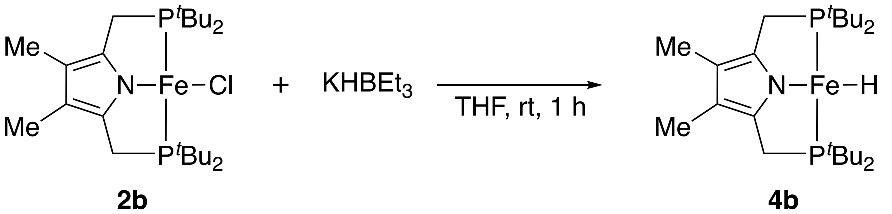

To a solution of **2b** (147 mg, 0.293 mmol) in THF (8 mL) was added $KHBEt_3$ (1.0 M in THF, 290 μL, 0.29 mmol) at room temperature. The resultant brown mixture was stirred at room temperature for 1 h, and the solvent was removed *in vacuo*. After the addition of Et_2O (7 mL) to the brown residue, the solution was filtered through Celite. The filtrate was concentrated to *ca.* 2 mL and the solution was kept at -30 °C to give **4b** as brown crystals, which were collected by decantation and dried *in vacuo* (22.4 mg, 0.0479 mmol, 16%). Brown crystals of **4b** suitable for X-ray crystallography were obtained by recrystallization from Et_2O at -30 °C. ^1H NMR (C_6D_6): 59.9, -14.8, -16.0. Magnetic susceptibility (Evans' method): $\mu_{eff} = 3.2\pm0.1$ μ_B in C_6D_6 at 298K. IR (KBr, cm^{-1}) 1671 (ν_{FeH}). Anal. Calcd. for $C_{24}H_{47}FeNP_2$: C, 61.67; H, 10.14; N, 3.00. Found: C, 60.86; H, 10.45; N, 2.51.

Reaction of 3b with KC_8.

To a mixture of **3b** (20.0 mg, 0.0074 mmol) and KC_8 (2.3 mg, 0.017 mmol) was added Et_2O (1 mL) under N_2 (1 atm) and the resultant red mixture was stirred at room temperature for 10 min. After benzene (3 mL) was added to the mixture, the solution was filtered through Celite. The filtrate was evaporated and dried *in vacuo* to afford a purple solid. The solid was dissolved in C_6D_6 containing naphthalene as an internal standard and the integration of ^{1}H NMR resonances revealed the formation of **1b** in 20% yield and **4b** in 52% yield.

^{1}H, ^{13}C{^{1}H} and ^{31}P{^{1}H} NMR spectra.

2,5-bis(dimethylaminomethyl)-3,4-dimethylpyrrole

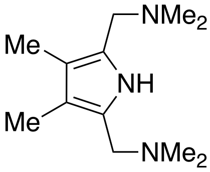

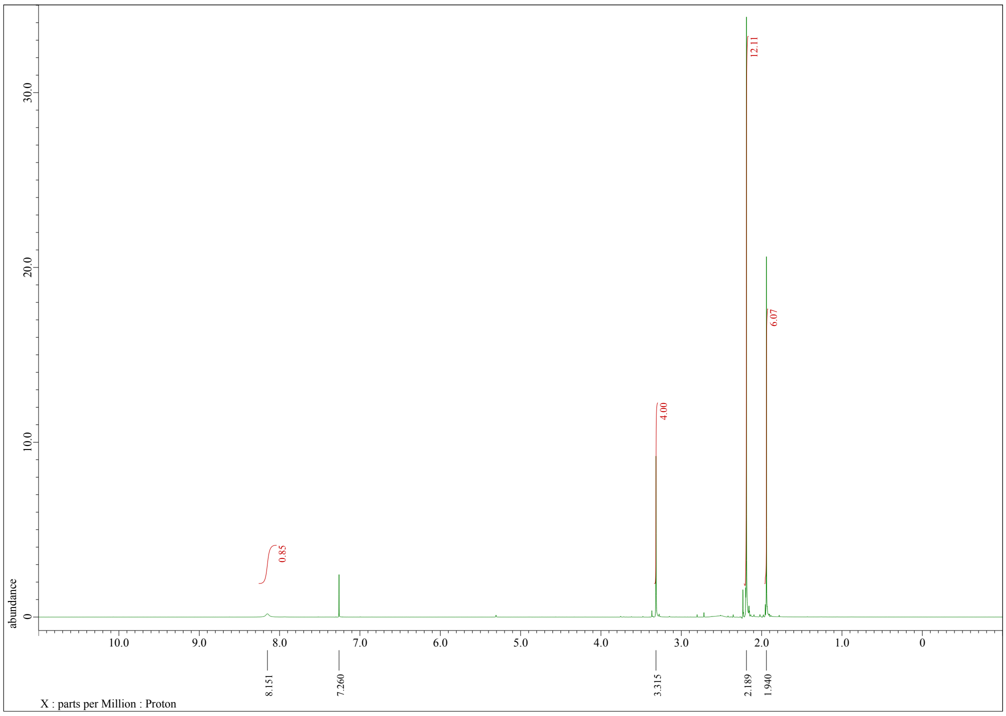

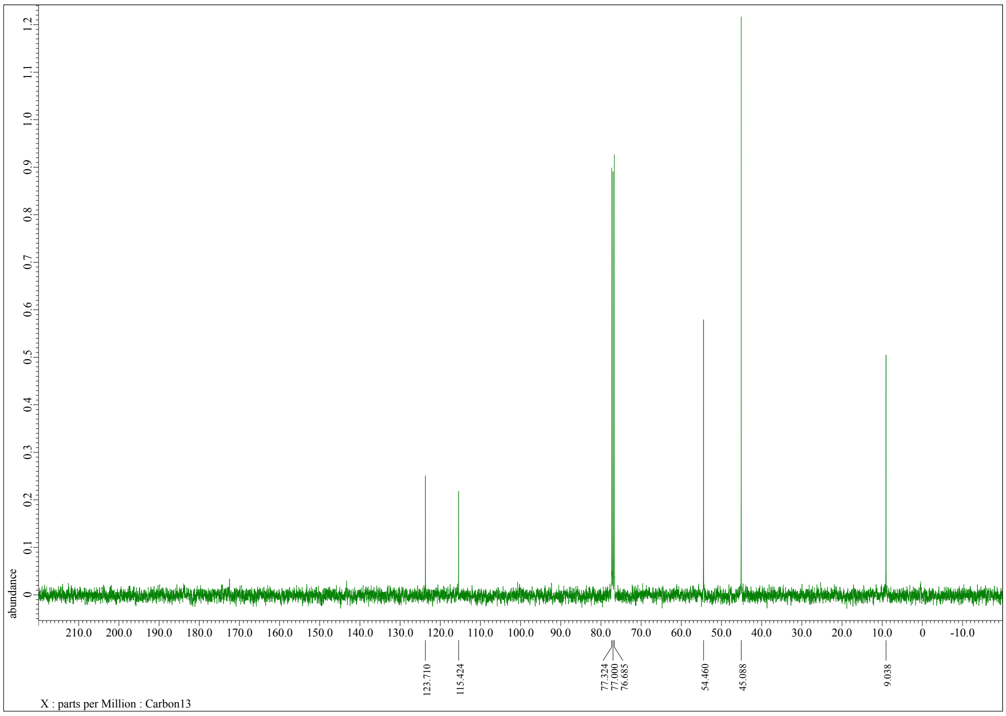

2,5-bis(di-*tert*-butylphosphinomethyl)-3,4-dimethylpyrrole

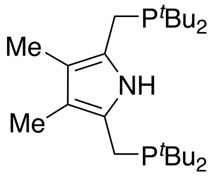

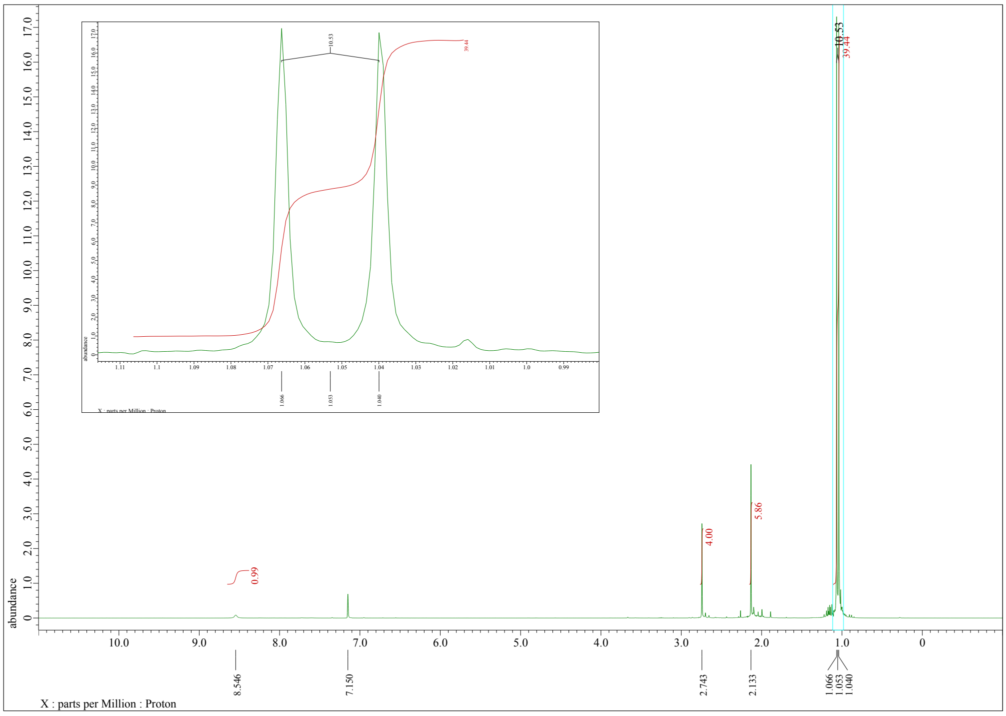

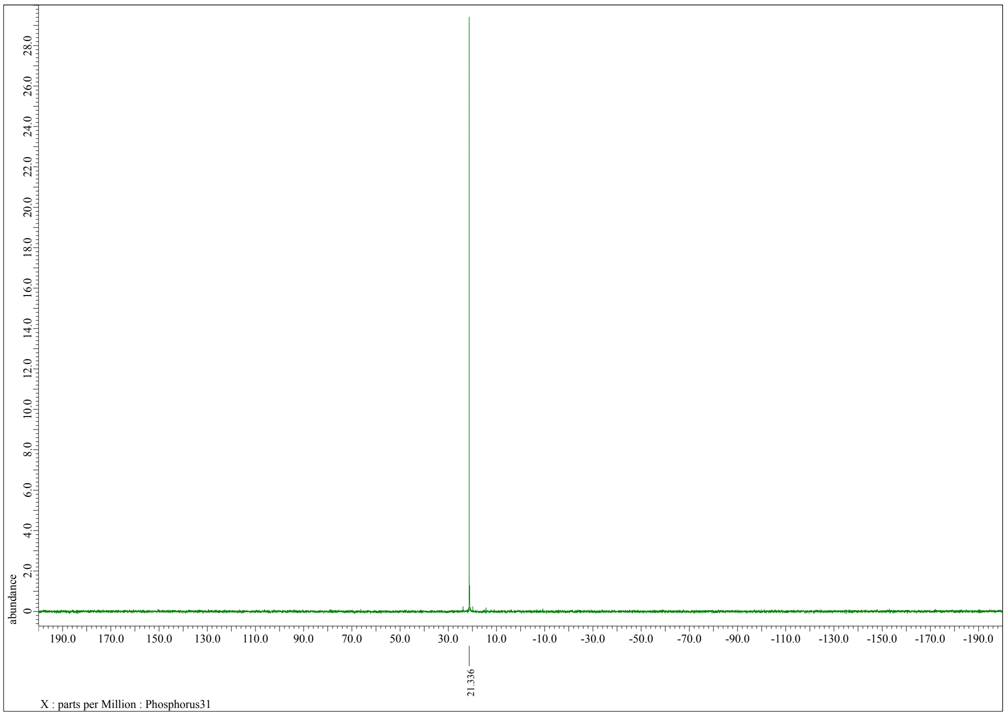

2,5-bis(di-*tert*-butylphosphinomethyl)-3,4-diphenylpyrrole

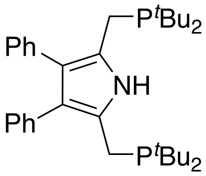

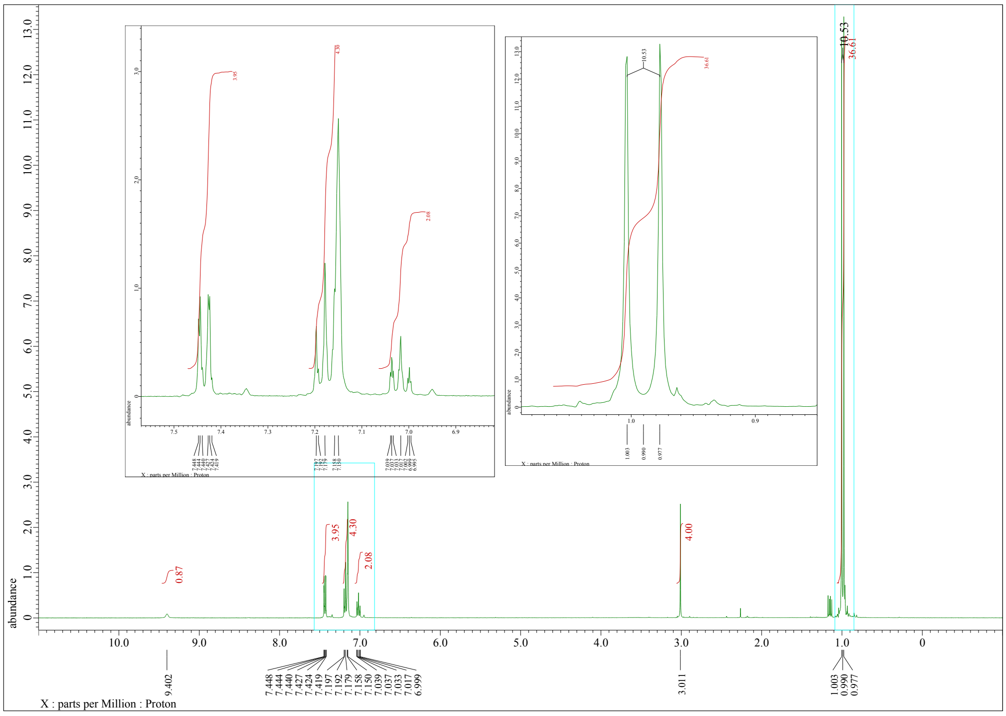

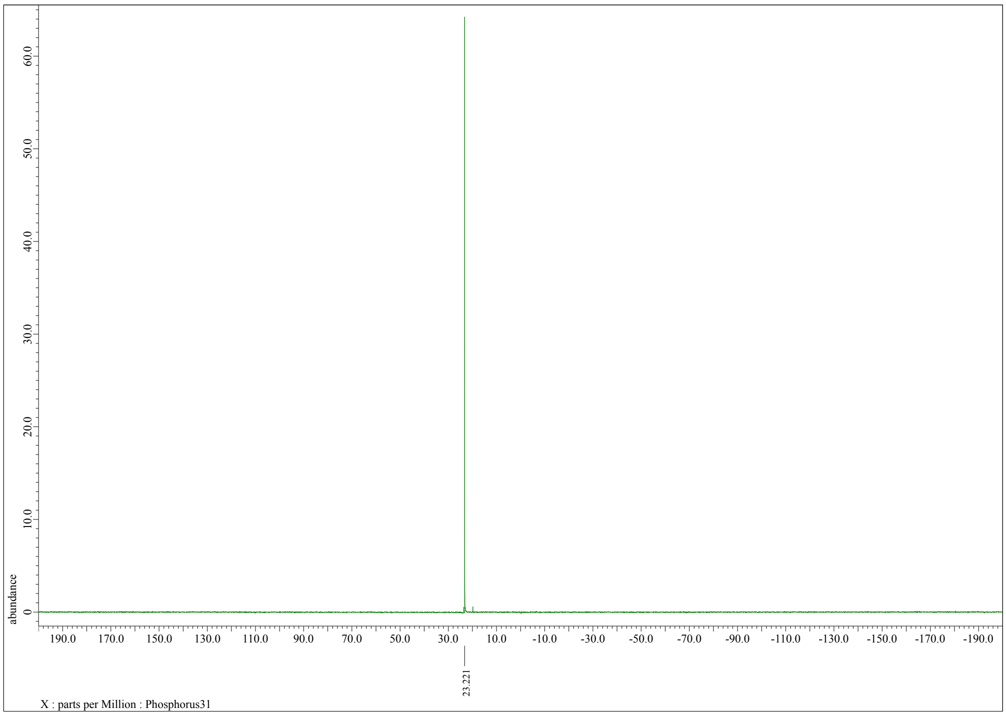

lithium 2,5-bis(di-*tert*-butylphosphinomethyl)-3,4-diphenylpyrrolide (Ph-PNP-Li)

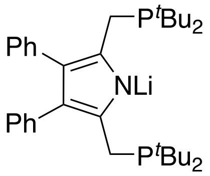

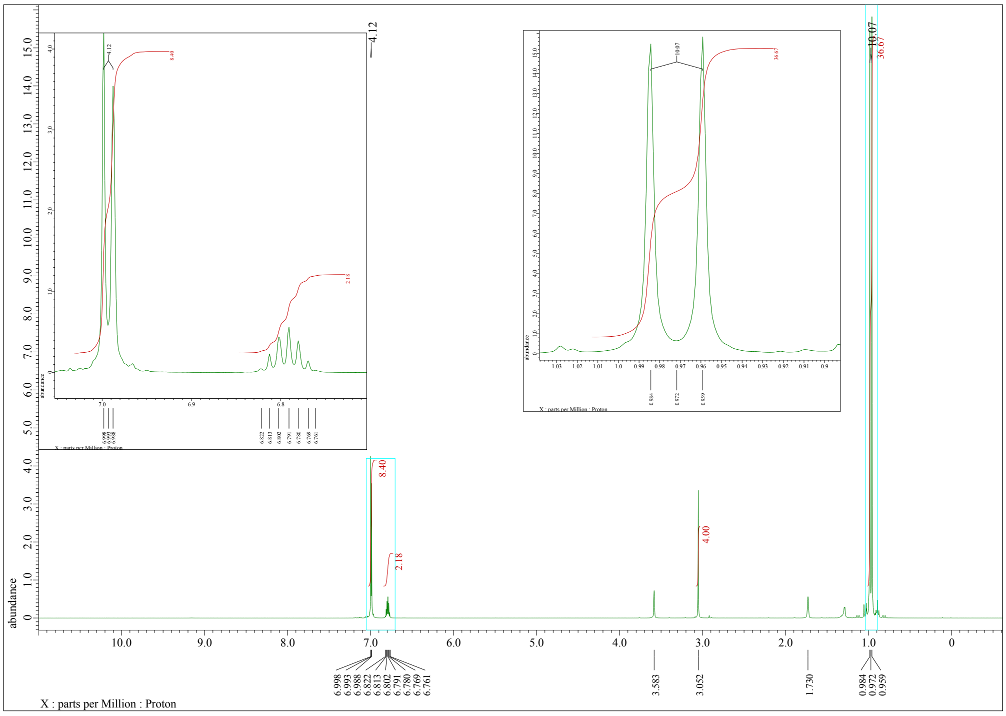

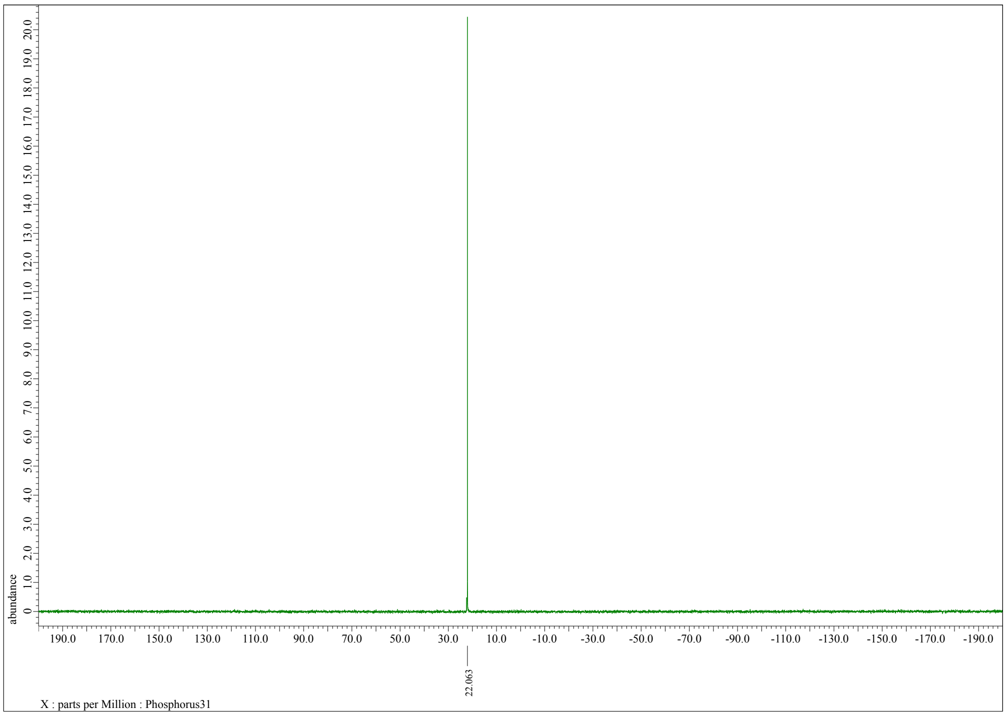

X-ray crystallography.

Crystallographic data of **2b**, **2c**, **1b**, **1c**, **3a**, **3b**·Et_2O and **4b** are summarized in Tables S1–S3. The ORTEP drawings of **2b**, **2c**, **1b**, **1c**, **3a**, **3b**·Et_2O and **4b** are shown in Figures S1–S7, and selected bond lengths and angles of **2b**, **2c**, **1b**, **1c**, **3a**, **3b**·Et_2O and **4b** are summarized in Tables S4–S10. Diffraction data for **2b**, **2c**, **1b**, **1c**, **3a**, **3b**·Et_2O and **4b** were collected for the 2θ range of 4° to 55° at –100 °C on a Rigaku RAXIS RAPID imaging plate area detector with graphite-monochromated Mo $K\alpha$ radiation (λ = 0.71075 Å) with VariMax optics. Intensity data were corrected for Lorenz-polarization effects and for empirical absorption (ABSCOR). The structure solution and refinements were carried out by using the *CrystalStructure* crystallographic software package.[12] The positions of the non-hydrogen atoms were determined by direct methods (SIR 97[13] for **2b**, **2c**, **1b**, **1c**, **3b**·Et_2O and **4b**; SHELXS Version 2013/1[14] for **3a**) and subsequent Fourier syntheses (SHELXL Version 2016/6[14]), and were refined on F_o^2 using all unique reflections by full-matrix least-squares with anisotropic thermal parameters except for some carbon, oxygen, and fluorine atoms in **3a** and **3b**·Et_2O. Two fluorine atoms in the BAr^F_4 anion of **3a** are disordered among two positions (F(8) and F(25), F(9) and F(26), each solved with atom occupancies of 0.6 and 0.4, respectively), thus were solved with isotropic thermal parameters. The ethereal atoms of **3b**·Et_2O (O(1), C(113), C(114), C(115) and C(116)) are slightly disordered thus were solved with isotropic thermal parameters. Crystals of **3a** also contain several solvent molecules which are too highly disordered to solve, thus PLATON/SQUEEZE methodology[15] has been applied to crystal data of **3a** (void size ~ 296 Å^3). All the hydrogen atoms were placed at the calculated positions with fixed isotropic parameters, except for the H(2) atom in **4b**. The position of the H(2) atom in **4b** was determined on an appropriate peak in the difference Fourier maps and further refined isotropically.

Table S1 | X-ray crystallographic data for 2b and 2c

	2b	**2c**
chemical formula	$C_{24}H_{46}ClFeNP_2$	$C_{34}H_{50}ClFeNP_2$
CCDC number	1552141	1552142
formula weight	501.88	626.02
dimensions of crystals, mm^3	0.55 × 0.07 × 0.02	0.15 × 0.15 × 0.10
crystal color, habit	orange, platelet	orange, block
crystal system	monoclinic	orthorhombic
space group	$P2_1/c$	$P2_12_12_1$
a, Å	7.9348(3)	12.1149(4)
b, Å	30.5114(10)	14.9649(5)
c, Å	11.7516(5)	18.4913(6)
α, deg	90	90
β, deg	106.870(8)	90
γ, deg	90	90
V, $Å^3$	2722.6(2)	3352.4(2)
Z	4	4
ρ_{calcd}, g cm^{-3}	1.224	1.240
$F(000)$	1080.00	1336.00
μ, cm^{-1}	7.797	6.473
trans. factors range	0.724 – 0.985	0.631 – 0.937
no. reflections measured	26155	33304
no. unique reflections	6237 (R_{int} = 0.0637)	7660 (R_{int} = 0.1060)
no. parameters refined	262	352
$R1$ ($I > 2\sigma(I)$)[a]	0.0431	0.0538
$wR2$ (all data)[b]	0.1008	0.1366
GOF (all data)[c]	1.027	1.031
max diff peak / hole, e $Å^{-3}$	+0.46 / –0.42	+0.52 / –0.55
Flack parameter		0.016(15)

[a] $R1 = \Sigma||F_o|-|F_c||/\Sigma|F_o|$. [b] $wR2 = [\Sigma w(F_o^2-F_c^2)^2/\Sigma w(F_o^2)^2]^{1/2}$, $w = 1/[\sigma^2(F_o^2) + (qP)^2 + rP]$, $P = (\mathrm{Max}(F_o^2, 0) + 2F_c^2)/3$ [q = 0.0483 (**2b**), 0.0613 (**2c**); r = 0.7507 (**2b**), 0 (**2c**)]. [c] GOF $= [\Sigma w(F_o^2-F_c^2)^2/(N_o-N_{params})]^{1/2}$.

Table S2 | X-ray crystallographic data for 1b, 1c and 3a

	1b	**1c**	**3a**
chemical formula	$C_{24}H_{46}FeN_3P_2$	$C_{34}H_{50}FeN_3P_2$	$C_{54}H_{55}BF_{24}FeN_3P_2$
CCDC number	1552143	1552144	1565341
formula weight	494.44	618.58	1330.61
dimensions of crystals, mm^3	0.18 × 0.08 × 0.06	0.15 × 0.05 × 0.01	0.25 × 0.10 × 0.05
crystal color, habit	purple, needle	purple, platelet	green, platelet
crystal system	monoclinic	orthorhombic	triclinic
space group	$P2_1/c$	$P2_12_12_1$	$P\bar{1}$
a, Å	7.9977(9)	11.3469(15)	12.2583(15)
b, Å	30.408(4)	12.4305(17)	12.4893(14)
c, Å	11.7607(14)	23.789(3)	21.819(3)
α, deg	90	90	87.436(6)
β, deg	106.780(8)	90	73.611(5)
γ, deg	90	90	88.777(6)
V, Å^3	2738.4(6)	3355.4(8)	3201.3(7)
Z	4	4	2
ρ_{calcd}, g cm^{-3}	1.199	1.224	1.380
$F(000)$	1068.00	1324.00	1354.00
μ, cm^{-1}	6.821	5.707	3.911
trans. factors range	0.324 – 0.960	0.500 – 0.994	0.089 – 0.981
no. reflections measured	24101	32962	28949
no. unique reflections	6281 (R_{int} = 0.1219)	7653 (R_{int} = 0.1032)	14219 (R_{int} = 0.1686)
no. parameters refined	285	361	776
$R1$ ($I > 2\sigma(I)$)[a]	0.1180	0.0539	0.1199
$wR2$ (all data)[b]	0.2874	0.1271	0.2333
GOF (all data)[c]	0.999	1.059	1.001
max diff peak / hole, e Å^{-3}	+1.57 / –1.12	+0.37 / –0.48	+0.69 / –0.36
Flack parameter		0.000(15)	

[a] $R1 = \Sigma||F_o|-|F_c||/\Sigma|F_o|$. [b] $wR2 = [\Sigma w(F_o^2-F_c^2)^2/\Sigma w(F_o^2)^2]^{1/2}$, $w = 1/[\sigma^2(F_o^2) + (qP)^2 + rP]$, $P = (\mathrm{Max}(F_o^2, 0) + 2F_c^2)/3$ [q = 0 (**1b**), 0.0505 (**1c**), 0 (**3a**); r = 43 (**1b**), 0 (**1c**), 9.7 (**3a**). [c] $\mathrm{GOF} = [\Sigma w(F_o^2-F_c^2)^2/(N_o-N_{\mathrm{params}})]^{1/2}$.

Table S3 | X-ray crystallographic data for 3b·Et$_2$O **and 4b**

	3b·Et$_2$O	**4b**
chemical formula	$C_{116}H_{128}B_2F_{48}Fe_2N_4OP_4$	$C_{24}H_{47}FeNP_2$
CCDC number	1565342	1565343
formula weight	2763.45	467.44
dimensions of crystals, mm^3	0.35 × 0.25 × 0.20	0.30 × 0.20 × 0.12
crystal color, habit	black, block	brown, block
crystal system	triclinic	monoclinic
space group	$P\bar{1}$	$C2/c$
a, Å	13.6593(3)	13.1139(15)
b, Å	19.7786(6)	19.901(2)
c, Å	25.3257(7)	11.5419(14)
α, deg	71.984(5)	90
β, deg	88.405(6)	115.595(8)
γ, deg	81.675(6)	90
V, Å^3	6437.0(4)	2716.6(6)
Z	2	4
ρ_{calcd}, g cm^{-3}	1.426	1.143
$F(000)$	2828.00	1016.00
μ, cm^{-1}	3.920	6.819
trans. factors range	0.750 – 0.925	0.183 – 0.921
no. reflections measured	62882	12228
no. unique reflections	29200 (R_{int} = 0.0469)	3111 (R_{int} = 0.0966)
no. parameters refined	1599	137
$R1$ ($I > 2\sigma(I)$)[a]	0.0857	0.0832
$wR2$ (all data)[b]	0.1828	0.1466
GOF (all data)[c]	1.011	1.000
max diff peak / hole, e Å^{-3}	+1.09 / –0.79	+0.72 / –0.66

[a] $R1 = \Sigma||F_o|-|F_c||/\Sigma|F_o|$. [b] $wR2 = [\Sigma w(F_o^2-F_c^2)^2/\Sigma w(F_o^2)^2]^{1/2}$, $w = 1/[\sigma^2(F_o^2) + (qP)^2 + rP]$, $P = (\text{Max}(F_o^2, 0) + 2F_c^2)/3$ [q = 0 (**3b**·Et$_2$O), 0 (**4b**),; r = 24 (**3b**·Et$_2$O), 19.5 (**4b**)]. [c] GOF = $[\Sigma w(F_o^2-F_c^2)^2/(N_o-N_{\text{params}})]^{1/2}$.

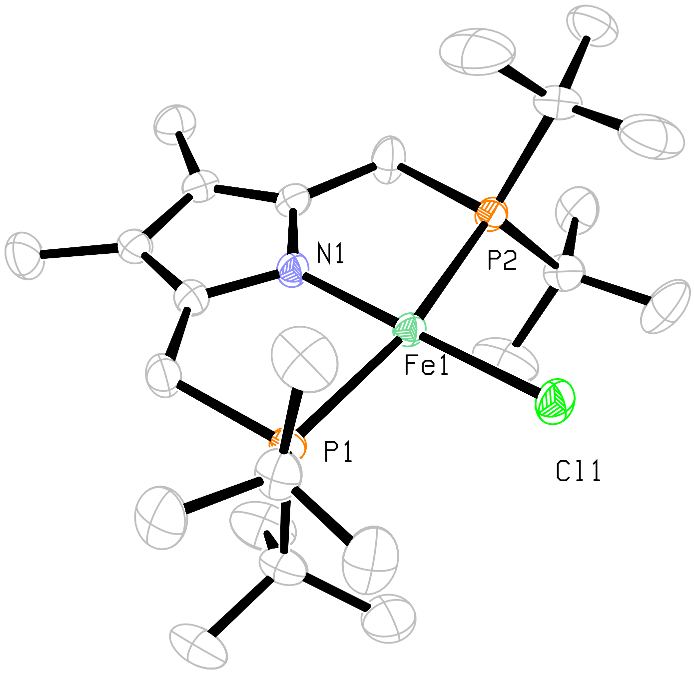

Figure S1. ORTEP drawing of **2b**. Thermal ellipsoids are shown at the 50% probability level. Hydrogen atoms are omitted for clarity.

Table S4. Selected Bond Lengths (Å) and Angles (deg) for **2b**.

Fe(1)—N(1)	1.8848(17)
Fe(1)—P(1)	2.2954(6)
Fe(1)—P(2)	2.2952(6)
Fe(1)—Cl(1)	2.2464(6)
P(1)—Fe(1)—P(2)	165.29(3)
N(1)—Fe(1)—P(1)	82.88(6)
N(1)—Fe(1)—P(2)	83.44(6)
N(1)—Fe(1)—Cl(1)	177.89(6)
P(1)—Fe(1)—Cl(1)	96.97(2)
P(2)—Fe(1)—Cl(1)	96.89(2)

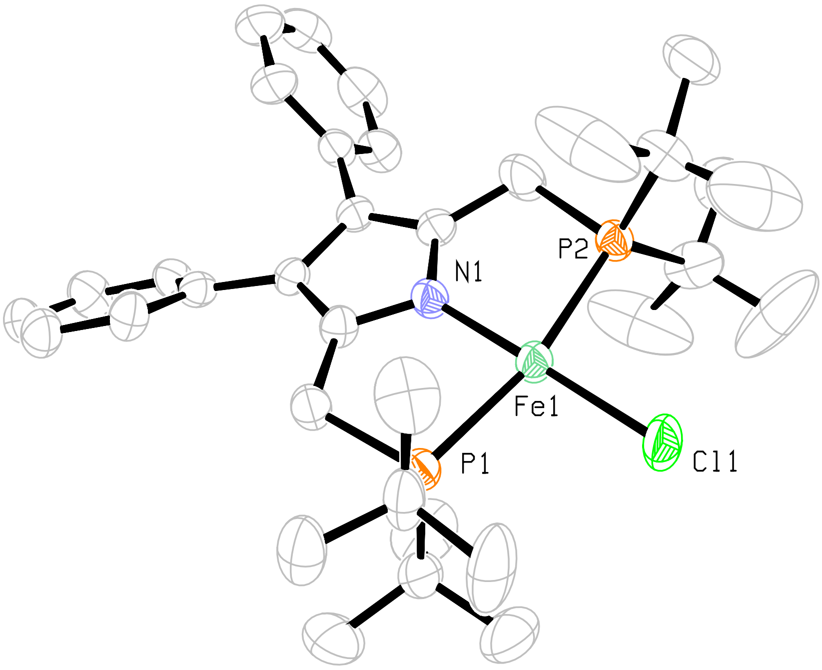

Figure S2. ORTEP drawing of **2c**. Thermal ellipsoids are shown at the 50% probability level. Hydrogen atoms are omitted for clarity.

Table S5. Selected Bond Lengths (Å) and Angles (deg) for **2c**.

Fe(1)—N(1)	1.905(4)
Fe(1)—P(1)	2.2884(13)
Fe(1)—P(2)	2.2942(13)
Fe(1)—Cl(1)	2.2361(14)
P(1)—Fe(1)—P(2)	166.86(5)
N(1)—Fe(1)—P(1)	83.14(11)
N(1)—Fe(1)—P(2)	83.73(11)
N(1)—Fe(1)—Cl(1)	178.53(13)
P(1)—Fe(1)—Cl(1)	96.54(5)
P(2)—Fe(1)—Cl(1)	96.60(5)

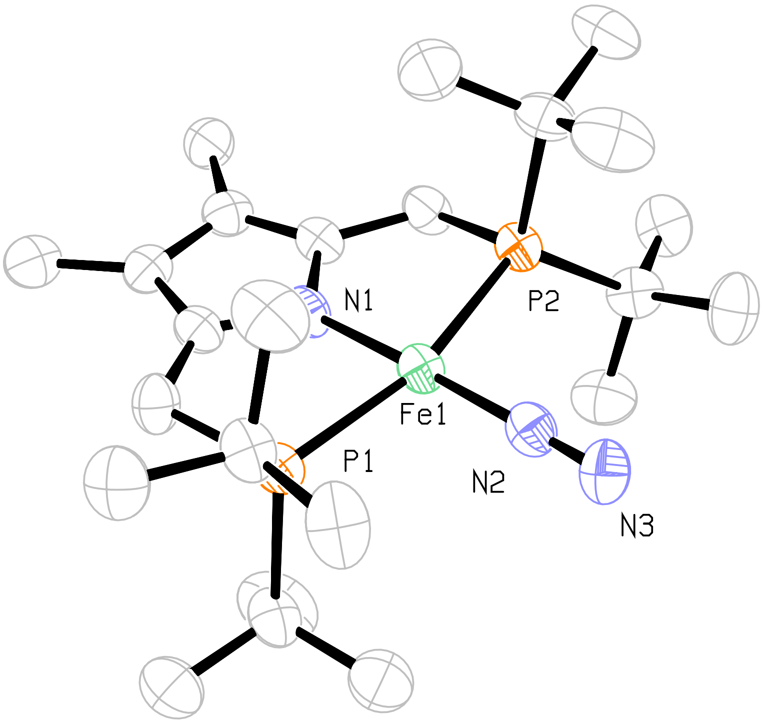

Figure S3. ORTEP drawing of **1b**. Thermal ellipsoids are shown at the 50% probability level. Hydrogen atoms are omitted for clarity.

Table S6. Selected Bond Lengths (Å) and Angles (deg) for **1b**.

Fe(1)—N(1)	1.909(7)
Fe(1)—P(1)	2.257(2)
Fe(1)—P(2)	2.266(2)
Fe(1)—N(2)	1.758(7)
N(2)—N(3)	1.136(9)
P(1)—Fe(1)—P(2)	164.69(9)
N(1)—Fe(1)—P(1)	83.0(2)
N(1)—Fe(1)—P(2)	82.4(2)
N(1)—Fe(1)— N(2)	177.6(3)
P(1)—Fe(1)— N(2)	96.6(2)
P(2)—Fe(1)— N(2)	98.1(2)
Fe(1)—N(2)— N(3)	179.0(8)

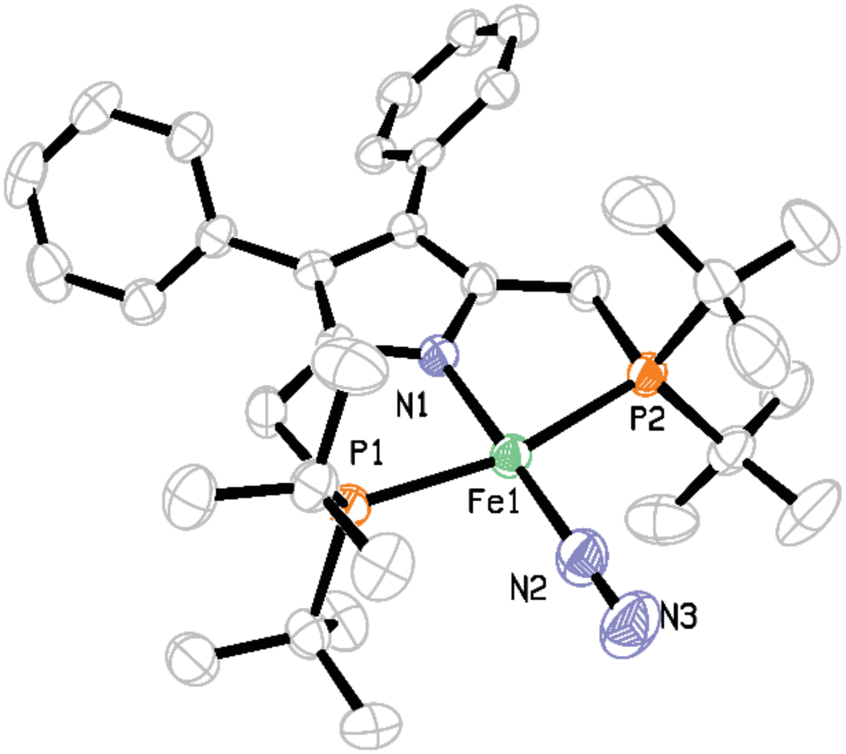

Figure S4. ORTEP drawing of **1c**. Thermal ellipsoids are shown at the 50% probability level. Hydrogen atoms are omitted for clarity.

Table S7. Selected Bond Lengths (Å) and Angles (deg) for **1c**.

Fe(1)—N(1)	1.924(4)
Fe(1)—P(1)	2.2534(15)
Fe(1)—P(2)	2.2483(15)
Fe(1)—N(2)	1.773(5)
N(2)—N(3)	1.124(6)
P(1)—Fe(1)—P(2)	166.21(6)
N(1)—Fe(1)—P(1)	83.29(13)
N(1)—Fe(1)—P(2)	83.33(12)
N(1)—Fe(1)— N(2)	176.8(2)
P(1)—Fe(1)— N(2)	97.33(16)
P(2)—Fe(1)— N(2)	96.21(16)
Fe(1)—N(2)— N(3)	178.0(6)

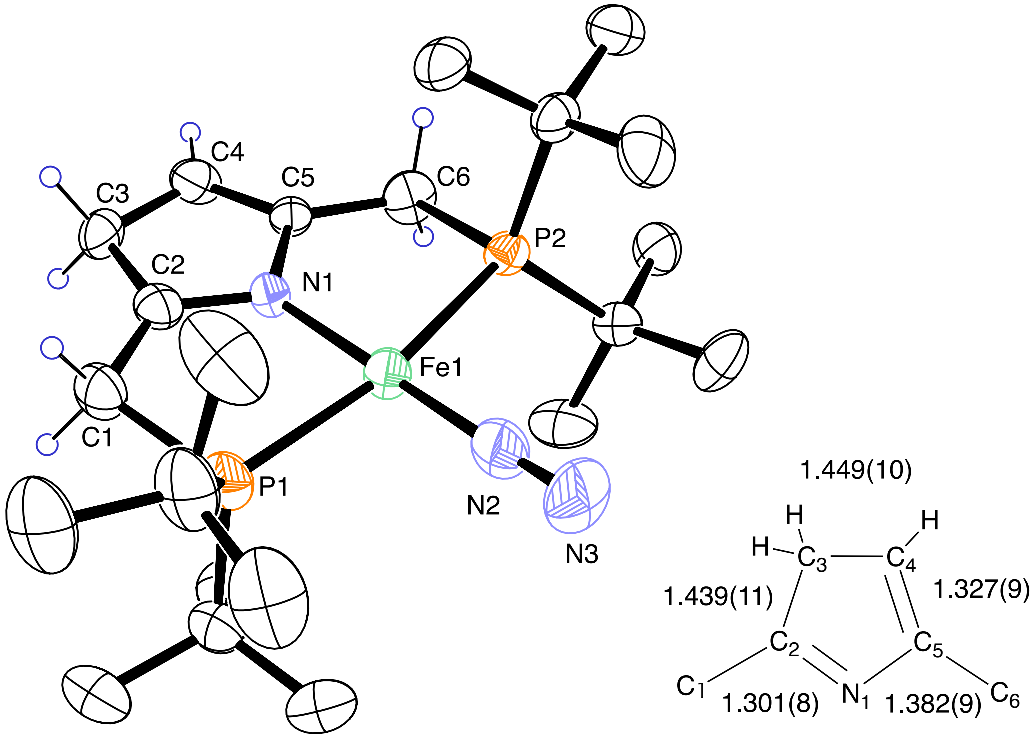

Figure S5. ORTEP drawing of **3a** and bond lengths (Å) of the protonated pyrrole ring. Thermal ellipsoids are shown at the 50% probability level. [BAr$^F{}_4$] moiety and hydrogen atoms of *tert*-butyl groups are omitted for clarity.

Table S8. Selected Bond Lengths (Å) and Angles (deg) for **3a**.

Fe(1)—N(1)	1.935(6)	N(1)—Fe(1)—P(2)	83.04(18)
Fe(1)—P(1)	2.264(2)	N(1)—Fe(1)— N(2)	178.6(4)
Fe(1)—P(2)	2.260(2)	P(1)—Fe(1)— N(2)	96.1(2)
Fe(1)—N(2)	1.770(9)	P(2)—Fe(1)— N(2)	97.5(2)
N(2)—N(3)	1.146(9)	Fe(1)—N(2)— N(3)	177.0(10)
N(1)—C(2)	1.301(8)	C(1)—C(2)— C(3)	127.0(7)
C(1)—C(2)	1.507(10)	C(1)—C(2)— N(1)	121.2(8)
C(2)—C(3)	1.439(11)	N(1)—C(2)— C(3)	111.8(7)
C(3)—C(4)	1.449(10)	C(2)—C(3)— C(4)	101.5(6)
C(4)—C(5)	1.327(9)	C(3)—C(4)— C(5)	108.7(7)
C(5)—N(1)	1.382(9)	C(4)—C(5)— N(1)	110.2(6)
C(5)—C(6)	1.503(10)	C(5)—N(1)— C(2)	107.8(6)
		C(4)—C(5)— C(6)	132.6(7)
P(1)—Fe(1)—P(2)	166.43(9)	N(1)—C(5)— C(6)	117.0(6)
N(1)—Fe(1)—P(1)	83.43(19)		

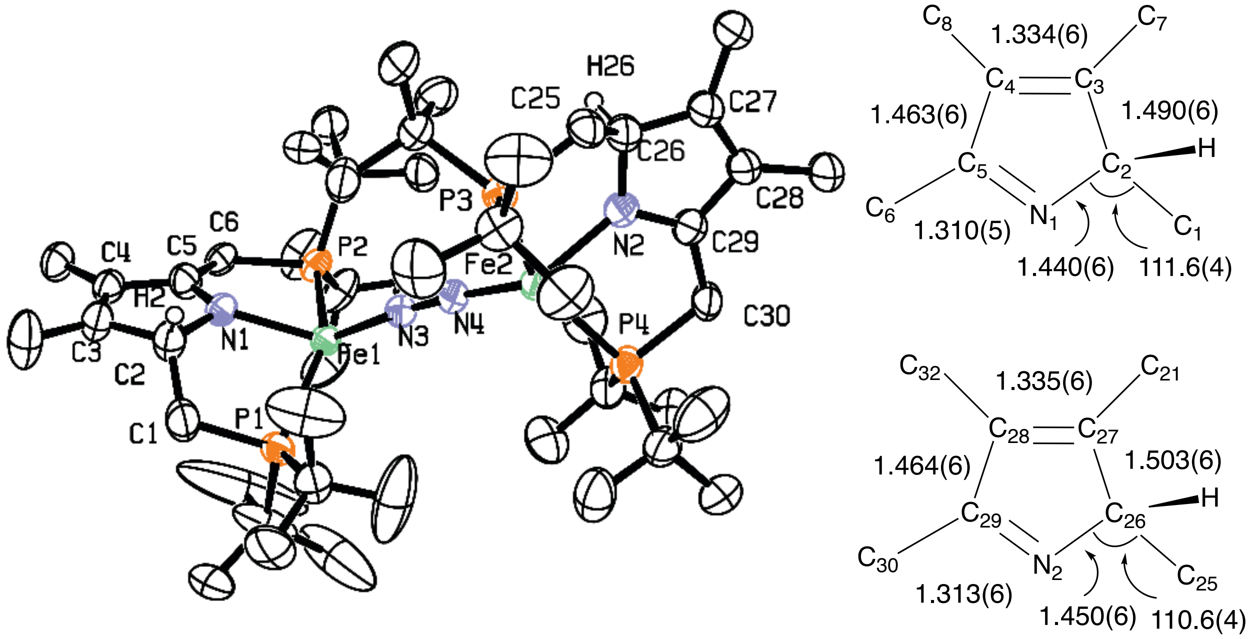

Figure S6. ORTEP drawing of **3b**·Et_2O and bond lengths (Å) and angles (deg) of the protonated pyrrole rings. Thermal ellipsoids are shown at the 50% probability level. Et_2O, $[BAr^F_4]_2$ moiety and hydrogen atoms except for H(2) and H(26) are omitted for clarity.

Table S9. Selected Bond Lengths (Å) and Angles (deg) for **3b**·Et_2O.

Fe(1)—N(1)	2.038(3)	Fe(2)—N(4)	1.803(4)	C(1)—C(2)—N(1)	111.6(4)
Fe(1)—P(1)	2.4080(13)	C(25)—C(26)	1.525(7)	C(1)—C(2)—C(3)	115.7(4)
Fe(1)—P(2)	2.4072(13)	C(26)—C(27)	1.503(6)	N(1)—C(2)—C(3)	105.9(4)
Fe(1)—N(3)	1.797(4)	C(27)—C(28)	1.335(6)	Fe(1)—N(3)—N(4)	175.7(3)
N(3)—N(4)	1.170(5)	C(28)—C(29)	1.464(6)	Fe(2)—N(4)—N(3)	173.8(4)
C(1)—C(2)	1.489(7)	C(29)—C(30)	1.472(6)	P(3)—Fe(2)—P(4)	147.57(5)
C(2)—C(3)	1.490(6)	C(29)—N(2)	1.313(6)	N(2)—Fe(2)—P(3)	82.29(11)
C(3)—C(4)	1.334(6)	N(2)—C(26)	1.450(6)	N(2)—Fe(2)—P(4)	80.54(11)
C(4)—C(5)	1.463(6)			N(2)—Fe(2)—N(4)	131.42(16)
C(5)—C(6)	1.483(6)	P(1)—Fe(1)—P(2)	144.11(5)	P(3)—Fe(2)—N(4)	105.94(12)
C(5)—N(1)	1.310(5)	N(1)—Fe(1)—P(1)	80.83(11)	P(4)—Fe(2)—N(4)	106.07(12)
N(1)—C(2)	1.440(6)	N(1)—Fe(1)—P(2)	80.77(10)	C(25)—C(26)—N(2)	110.6(4)
Fe(2)—N(2)	2.032(4)	N(1)—Fe(1)—N(3)	126.45(15)	C(25)—C(26)—C(27)	116.7(4)
Fe(2)—P(3)	2.4053(12)	P(1)—Fe(1)—N(3)	106.91(12)	N(2)—C(26)—C(27)	105.4(4)
Fe(2)—P(4)	2.4100(13)	P(2)—Fe(1)—N(3)	108.83(12)		

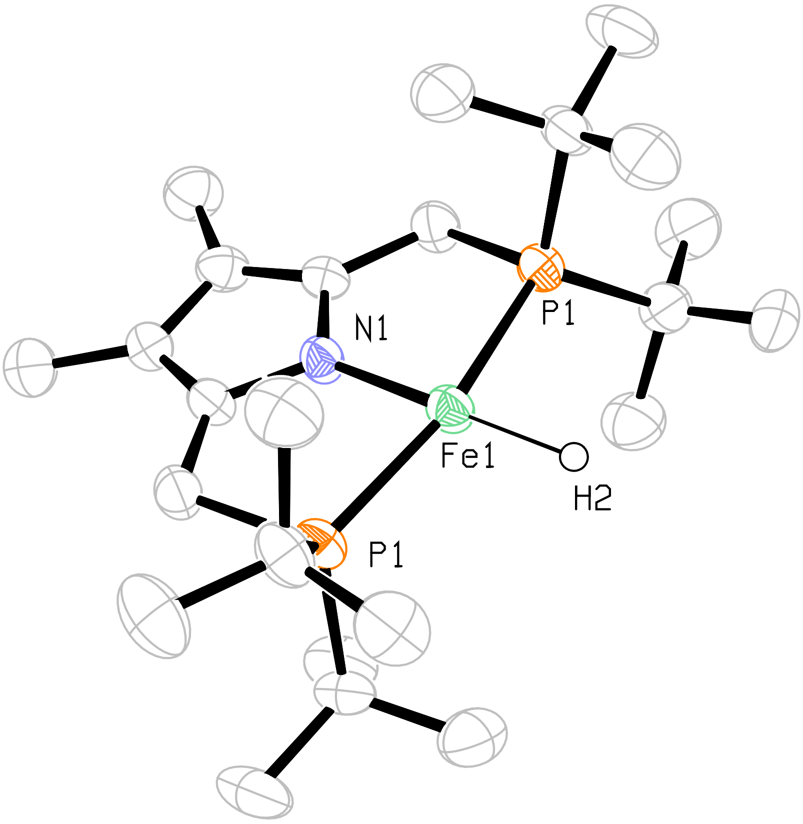

Figure S7. ORTEP drawing of **4b**. Thermal ellipsoids are shown at the 50% probability level. Hydrogen atoms except for H(2) are omitted for clarity.

Table S10. Selected Bond Lengths (Å) and Angles (deg) for **4b**.

Fe(1)—N(1)	1.906(5)
Fe(1)—P(1)	2.2356(11)
Fe(1)—H(2)	1.74(5)
P(1)—Fe(1)—P(1)	167.34(7)
N(1)—Fe(1)—P(1)	83.67(4)
N(1)—Fe(1)—H(2)	180.0
P(1)—Fe(1)— H(2)	96.33(4)

Electrochemical Study.

Cyclic voltammograms (CVs) were recorded on an ALS/Chi model 610C electrochemical analyzer with platinum working electrode in THF containing 1 mM of sample and 0.1 M of $[N^nBu_4]PF_6$ as a supporting electrolyte at a scan rate of 0.1 V/s at room temperature. All potentials were measured against an $Ag^{0/+}$ electrode and converted to the values vs $ferrocene^{0/+}$. The all cyclic voltammetric data of **1a**, **1b** and **1c** revealed irreversible reduction and irreversible oxidation.

Table S11. Cyclic voltammetric data and IR spectra for iron dinitrogen complexes **1a-1c**.

compound	E_{pa} (V)	E_{pc} (V)	ν_{NN} (cm^{-1})
1a	-0.72	-2.88	1964
1b	-0.76	-2.92	1959
1c	-0.63	-2.82	1969

References

1. Evans, D. F. *J. Chem. Soc.* **1959**, 2003.

2. Live, D. H.; Chan, S. I. *Anal. Chem.* **1970**, *42*, 791.

3. Bain, G. A.; Berry, J. F. *J. Chem. Educ.* **2008**, *85*, 532.

4. Kancharla, P.; Reynolds, K. A. *Tetrahedron* **2013**, *69*, 8375.

5. Nguyen, L. T.; Senge, M. O.; Smith, K. M. *J. Org. Chem.* **1996**, *61*, 998.

6. Kern, R. J. J. *Inorg. Nucl. Chem.* **1962**, *24*, 1105.

7. Weitz, I. S.; Rabinovitz, M. *J. Chem. Soc., Perkin Trans.* **1993**, *1,* 117.

8. Brookhart, M.; Grant, B.; Volpe, A. F. *Organometallics* **1992**, *11*, 3920.

9. Kuriyama, S.; Arashiba, K.; Nakajima, K.; Matsuo, Y.; Tanaka, H.; Ishii, K.; Yoshizawa, K.; Nishibayashi, Y. *Nat. Commun.* **2016**, *7*, 12181.

10. Weatherburn, M. W. *Anal. Chem.* **1967**, *39*, 971.

11. Watt, G. W.; Chrisp, J. D. *Anal. Chem.* **1952**, *24*, 2006.

12. *CrystalStructure 4.22*: *Single Crystal Structure Analysis Software*; Rigaku Corp: Tokyo, Japan, and MSC: The Woodlands, TX, 2016.

13. Altomare, A.; Burla, M. C.; Camalli, M.; Cascarano, G. L.; Giacovazzo, C.; Guagliardi, A.; Moliterni, A. G. G.; Polidorib, G.; Spagnac, R. *J. Appl. Crystallogr.* **1999**, *32*, 115–119.

14. Sheldrick, G. M. *Acta crystallogr.* **2008**, *A64*, 112-122.

15. Spek, A. L. *PLATON: A Multipurpose Crystallographic Tool.* Utrecht University: Utrecht, The Netherlands, 1998.